THE DYNAMIC RESPONSE OF BRAIN TEMPERATURE TO LOCALIZED HEATING

K. G. KASTELLA *and* JAMES R. FOX

From the Department of Physiology and Biophysics, University of Washington School of Medicine, Seattle, Washington 98105. Dr. Kastella's present address is the Department of Physiology, School of Medicine, University of New Mexico, Albuquerque, New Mexico 87106.

ABSTRACT Several mathematical descriptions of heat transport in perfused tissues have been proposed but have not been thoroughly tested under conditions of time-varying temperatures. Data was obtained by measuring the response of brain temperature to step changes in temperature of chronically implanted thermodes in conscious baboons. These responses were compared to numerical solutions of an equation expressing heat transport in terms of conduction in the tissue and convection due to capillary blood flow. Good agreement between experimental and theoretical curves was obtained for values of k (thermal diffusivity) of 0.0017–0.0021 cm^2/sec and ϕ (blood flow per unit volume of tissue) of 0.3–0.7 cm^3/cm^3-min. The predicted temperature response at a given tissue location was not greatly affected either by changes in k and ϕ over the physiological range, or by small errors in describing experimental geometry. However, inaccuracies in describing boundary locations or failing to account for the relatively avascular scar tissue around the thermode changed the value of ϕ needed to fit the data by as much as 50%. Thus, we conclude that the model described in this paper can be used for a description of thermal gradients surrounding a thermode but extreme caution should be exercised if such a model is used to quantitatively evaluate blood flow.

INTRODUCTION

Heat transport from heated or cooled probes implanted in brain tissue results from conduction through the tissue and convection due to blood flow. The parameters associated with conduction have been measured using nonliving tissue (Ponder, 1962; Chato and Shitzer, 1970; Cooper and Trezek, 1970), while the effect of blood flow has been studied mainly in conjunction with the evaluation of thermal methods of measuring tissue perfusion (Gibbs, 1933; Grayson, 1952; Betz, 1965; among others). Since the purpose of many studies performed in vivo was to determine empirically a method of measuring local blood flow, little effort has been spent evaluating the quantitative effect of convection and conduction on thermal gradients. The model proposed by Perl (1962) treated heat transport in terms of conduction through a homogeneous medium and an additive term resulting from convec-

tive heat transport in blood. Similar models were reported by Rutkin and Barish (1964), and Jewett and Trezek (1967). These models were tested using only steady-state temperature fields. However, a system cannot be characterized completely by the steady-state response.

The purpose of this study was fourfold: (*a*) to measure the dynamic changes in brain temperature using an implanted thermode; (*b*) to determine if the dynamic data is in agreement with previously reported models; (*c*) to evaluate the parameters associated with conduction and convection which determine temporal and spatial temperature distribution; and (*d*) to find the sensitivity of temperature to the above parameters, and thus assess the possibility of quantitatively measuring regional brain blood flow using thermal techniques.

EXPERIMENTAL METHODS

All experiments were performed on unanesthetized, chair-restrained baboons (*Papio anubis*). The disturbing effects of the laboratory environment were minimized by conducting all experiments while the animal was in a sound-deadened room (Industrial Acoustics Co., Inc., Bronx, N. Y.).

A water-perfused thermode, capable of producing various temperature wave forms, was used to vary brain temperature. Details of the thermode and control circuit have been described elsewhere (Kastella, 1970). Briefly, the thermode consists of two gold-plated stainless steel needles (1.066 mm O.D.) implanted stereotaxically, with the needle tips located bilaterally (3 mm to either side of the midline) in the preoptic/anterior hypothalamic area. Three thermocouple probes, consisting of 40-gauge, copper-constantan thermocouples inside a length of 26-gauge stainless steel hypodermic stock (0.47 mm O.D.) were used for temperature measurements. One thermocouple probe was soldered to the side of each thermode needle; the remaining thermocouple probe was located in hypothalamic tissue approximately 2 mm behind the right-hand thermode needle. The three thermocouple beads were located in approximately the same horizontal plane, i.e., 1–2 mm above the tip of the thermode needles. The thermode needle–thermocouple probe assembly was packaged as a single unit.

Temperature at the thermode tip was controlled by means of a negative feedback control circuit. The feedback signal was provided by the amplified voltage from one of the thermode tip thermocouples. After filtering, the feedback signal was compared with the desired input wave form and the difference voltage fed into a power amplifier, which in turn drove a small heater. The heater, an integral part of the thermode-thermocouple assembly, was located in a chamber chronically attached to the top of the animal's skull.

Temperature in the hypothalamic tissue and temperature at the tip of one of the two thermode needles could be measured simultaneously. At a water flow rate of approximately 50 ml/min, sine or square wave temperature variations could be produced over the frequency range 0.001–0.05 Hz with a maximum peak-to-peak amplitude of 8°C (measured at the tip of the thermode).

The thermode was implanted under aseptic conditions with the aid of an X-ray stereotaxic frame (Mechanical Developments Co., South Gate, Calif.). X-rays taken during the implant were used to insure placement of the thermode tips in the preoptic/anterior hypothalamic area and for accurate measurement of the geometrical relationship between thermocouples and thermode.

When sacrificed, the animals were anesthetized with Nembutal and the upper body and head were perfused through the left ventricle of the heart with 10% formalin solution. The brain was removed and frozen; 50-μ-thick sections were made and stained with cresyl violet. Thermode position and tissue damage was determined by gross and microscopic examination of the sections.

THEORETICAL CONSIDERATIONS

A mathematical description of heat transport in living tissue should account for heat conduction through the tissue, heat convection due to blood flow, and heat production due to metabolism. A partial differential equation describing these processes in terms of independent additive effects of conduction, convection, and metabolic heat production was proposed by Brown (1965):

$$\frac{\partial}{\partial t}\rho cT = \text{div } K \text{ grad } T - \text{div } \rho_b c_b T\mathbf{q} + h_m, \qquad (1)$$

where

ρ = tissue density (g/cm^3),
c = tissue specific heat (cal/g-°C),
K = tissue thermal conductivity (cal/°C-cm-sec),
$\mathbf{q}$ = blood velocity vector (cm/sec),
ρ_b = blood density (g/cm^3),
c_b = blood specific heat (cal/g-°C),
h_m = metabolic heat production (cal/cm^3-sec),
T = temperature (°C).

Exact solution of equation 1 requires knowledge, over all time, of the specific heats, densities, and thermal conductivities of blood and tissue, as well as blood velocity for each point in the tissue.

Perl (1962) applied a special case of equation 1, expressed as a difference equation, to finite volume elements. With this approach, the average tissue and blood properties for each volume element may be used in the equation provided that the size of the volume element is properly chosen. The volume element must be small enough for customary mathematical methods of calculus to hold, and for temperature throughout the element to be considered uniform; yet the volume element must be large enough, relative to the formed components within it, that the thermal properties do not vary significantly from element to element, thus allowing characterization in terms of average properties (Perl, 1962).

In Perl's formulation, the arterial blood entered an element at some temperature T_a, but, by the time the blood reached the capillaries, it was assumed to be in thermal equilibrium with the surrounding tissue. Thus, the convection term of equa-

tion 1 can be separated into two terms:

$$\text{div } \rho_b c_b T\mathbf{q} = \text{div } \rho_b c_b T\mathbf{q}_c - \rho_b c_b \phi(T_a - T), \tag{2}$$

where ϕ = arterial-to-capillary blood flow per unit volume of tissue (cm^3/cm^3-sec), and $\mathbf{q}_c$ = capillary blood velocity vector (cm/sec). In equation 2, the first term on the right represents heat flow through those capillaries which intersect the surface of the element (capillary heat convection), while the second term on the right represents equilibration of arterial blood temperature with the temperature of the element (forced convection).

Using the following two assumptions—(*a*) the density and specific heat of the tissue and blood are time- and space-invariant, and (*b*) capillary heat convection is insignificant (see Discussion)—and expressing the temperature at each point as the difference between the actual temperature and the initial temperature, equation 1 can be written as:

$$\frac{\partial T'}{\partial t} = \text{div } k \text{ grad } T' - \phi' T', \tag{3}$$

where $\phi' = \phi(\rho_b c_b/\rho c)$ = adjusted blood flow (sec^{-1}), k = tissue thermal diffusivity = $K/\rho c$ (cm^2/sec), and T' = change in tissue temperature (°C).

In most previous studies, only the steady-state solution to equation 3 has been obtained. Since such a solution depends only on the ratio of parameters ϕ':k, no unique value for either parameter can be obtained unless the other parameter is determined by independent measurements. By contrast, two parameters, k and ϕ', are needed to uniquely specify the solution to equation 3 for time-varying temperatures. Comparison of these solutions with experimental responses to dynamic temperature forcings will provide a more rigorous test of equation 3 and yield estimates for both k and ϕ'. If the equation is a good representation of heat transport, variations in blood flow will change computed values for ϕ' while having no effect on k. Thus, an important aspect of the model can be tested without an independent measure of ϕ'.

In addition to the parameters noted above, solution of equation 3 requires knowledge of the boundary and initial conditions (see Appendix I). The validity of the assumptions about the parameters and the initial and boundary conditions will be discussed later. As will be seen, the values computed for ϕ' and k from experimental data are very sensitive to these assumptions.

EXPERIMENTAL RESULTS

The temperature-forcing, defined as the thermode temperature as a function of time, consisted of step and sinusoidal changes in temperature. Examples of the tempera-

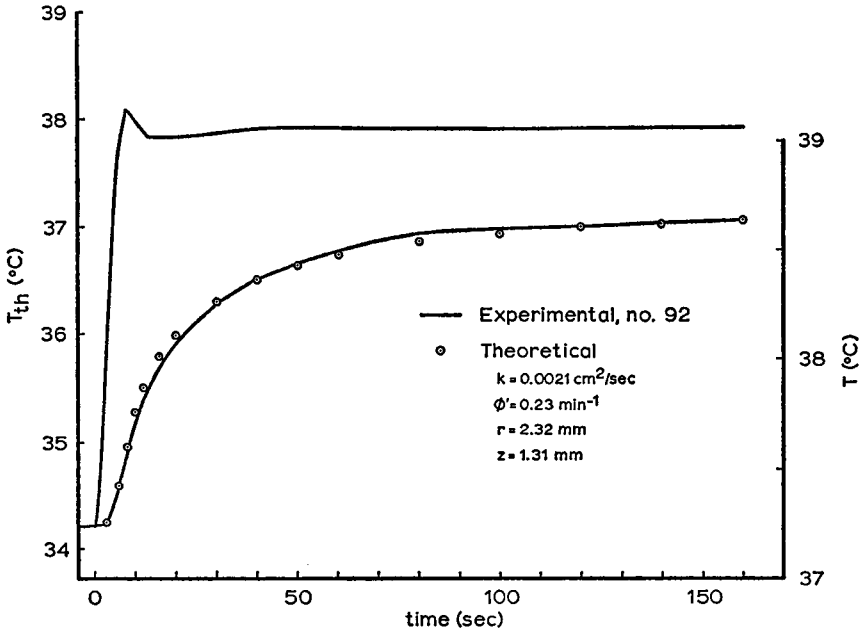

FIGURE 1 The response of tissue temperature (lower solid line and scale on the right) to a step increase in thermode temperature (upper solid line and scale on the left). The computer-simulated response is shown as open circles. Coordinates (with respect to the thermode tip) of tissue thermocouple and values for k and ϕ' used for solution of equation 3 are shown on the figure.

ture response at a remote point in brain tissue to a "step" increase in thermode temperature is shown as solid lines in Figs. 1, 5, and 6.

Examples of the experimental response to sinusoidal temperature-forcing are shown in Figs. 2 and 4. The response is expressed in terms of gain and phase for seven different forcing frequencies in the range of 0.001–0.05 Hz. Experimental gain was independent of the amplitude of the forcing function over the temperature range of 4–8°C (peak-to-peak).

Histological sections through the area occupied by the thermodes were cut from the brains of most experimental animals. A representative coronal section from the region of maximum tissue damage is shown in Fig. 3.

THEORETICAL RESULTS

A numerical solution of equation 3 in cylindrical coordinates was obtained using a difference equation approximation (refer to Appendix II). The experimental forcing function, sampled at 0.25 sec intervals, was used for the thermode boundary condition $f(t)$, $(t > 0)$ in the theoretical calculations. Temperature responses to the sampled step temperature-forcing were computed for coordinates corresponding to

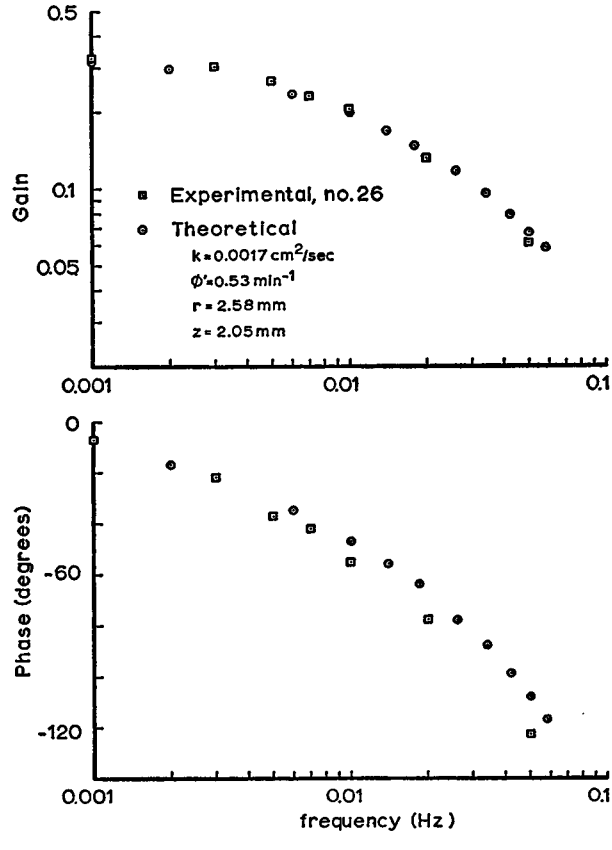

FIGURE 2 Response of tissue temperature to sinusoidal changes in thermode temperature (squares) and the simulated response (circles). Coordinates of tissue thermocouple and values for k and ϕ' used for solution of equation 3 are shown on the figure.

the remote thermocouple location and are shown as circles in Figs. 1 and 4. These curves represent the visually determined "best fit" between experimental and theoretical results (obtained by trying various values of k and ϕ') and were calculated using values of k and ϕ' shown in the figures.

To obtain theoretical data in the frequency domain the sampled step forcing function and computed response were Fourier-transformed using standard methods (Hamming, 1962), and gain and phase were computed from the Fourier coefficients. A plot of gain and phase vs. frequency for experimental and computed data is shown in Figs. 2 and 4. In each case values for k and ϕ' used for computation were those of providing a visual best fit to experimental data.

FIGURE 3 Coronal section through the region occupied by the thermode, illustrating the extent of tissue damage. (Cresyl violet stain.)

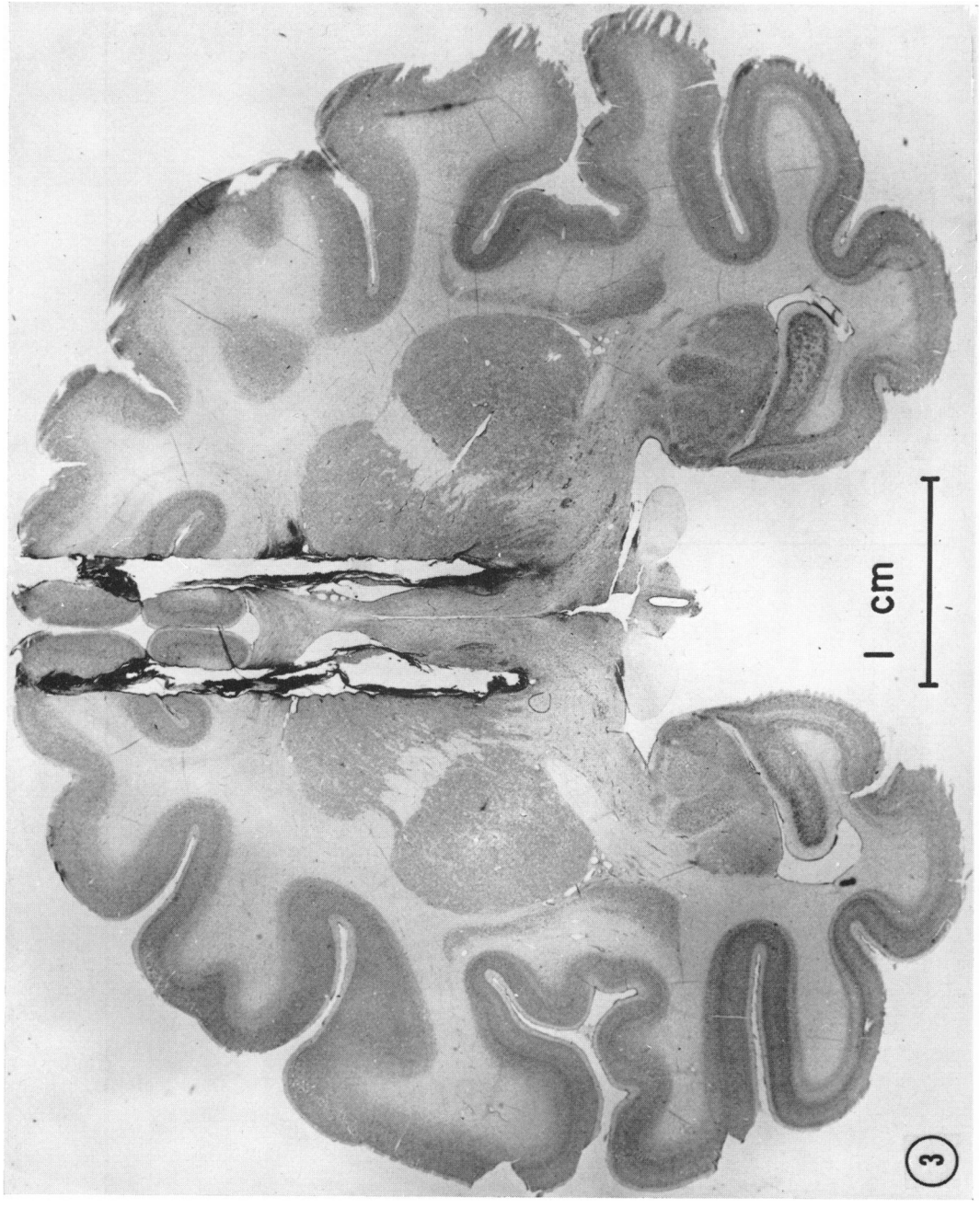
1 cm
3

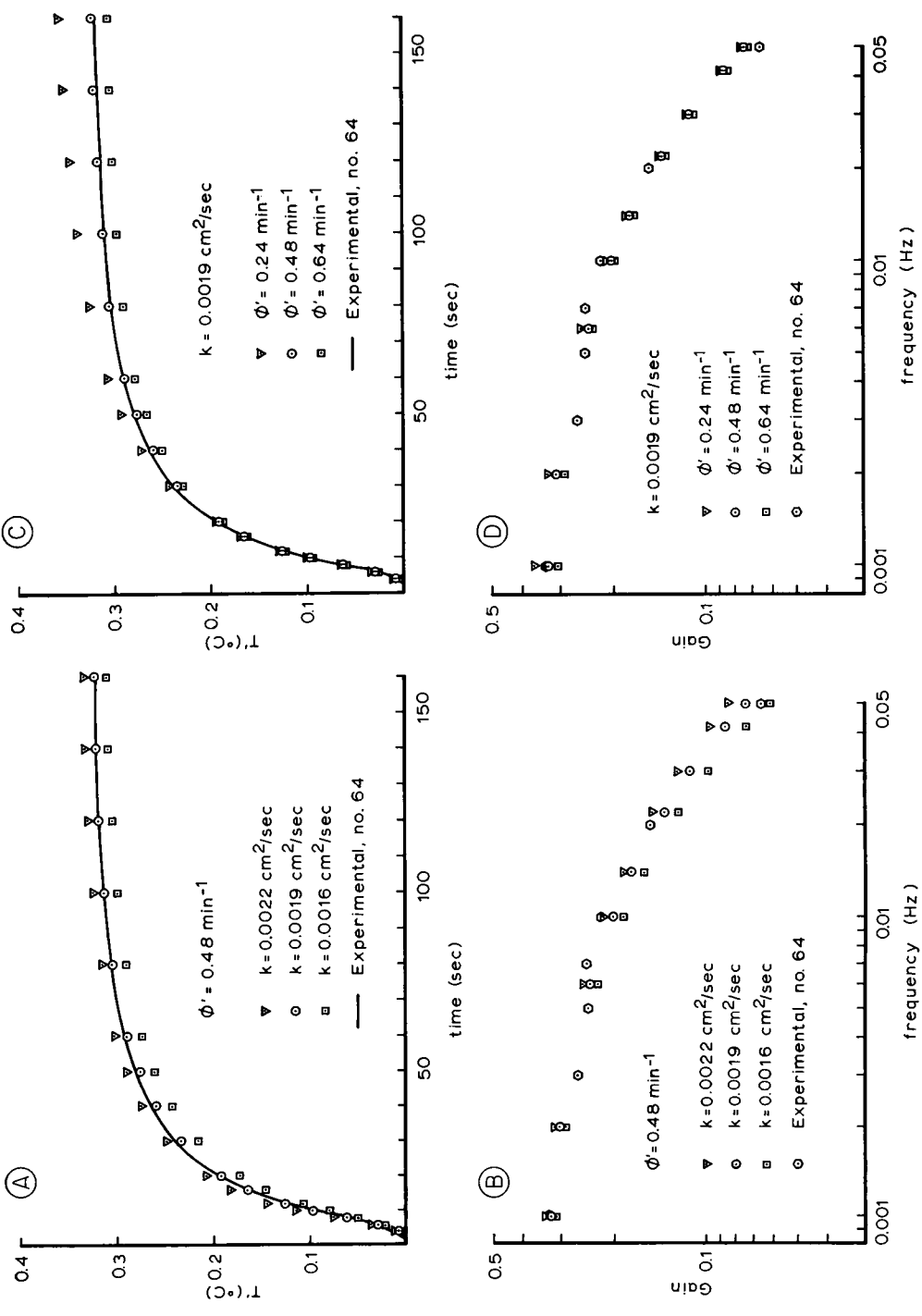
A
B
C
D
Φ' = 0.48 min⁻¹
k = 0.0022 cm²/sec
k = 0.0019 cm²/sec
k = 0.0016 cm²/sec
Experimental, no. 64
T'(°C)
time (sec)
Gain
frequency (Hz)
k = 0.0019 cm²/sec
Φ' = 0.24 min⁻¹
Φ' = 0.48 min⁻¹
Φ' = 0.64 min⁻¹

FIGURE 4

Two parameters, k and ϕ', were used to fit the experimental data. Values of k ranged from 0.0017 to 0.0021 cm²/sec, which is in reasonable agreement with previously reported values of 0.0011–0.0024 cm²/sec obtained from various tissues. The value of 0.0011 cm²/sec obtained by Trezek et al. (1968) was determined for living white matter, and, because of the high lipid content, would be expected to have a lower thermal diffusivity than gray matter. Ponder (1962) reported values of 0.0017–0.0019 cal/cm-°C-sec for thermal conductivity (K) in freshly excised brain slices. Using $\rho = 1.05$ g/cm³ and $c = 0.88$ cal/g-°C obtained from gray matter (Cooper and Trezek, 1970) gives values for thermal diffusivity ($K/\rho c$) of 0.0018–0.0021 cm²/sec. Thermal diffusivity of 0.0014 cm²/sec has been reported for gray matter from cadaver brains (Cooper and Trezek, 1970) and 0.0015–0.0018 cm²/sec for cat brain (Chato and Shitzer, 1970).

Values of ϕ' used to fit the experimental data ranged from 0.3 to 0.7 min^{-1}. Using $\rho_b = 1.06$ g/cm³, $c_b = 0.86$ cal/g-°C (Mendlowitz, 1948), and values of ρ and c mentioned above, yields estimates of ϕ from 0.3 to 0.7 ml/ml-min, which agrees favorably with reported values of blood flow in the cerebral cortex of the anesthetized baboon (James et al., 1969), hypothalamus of the conscious rabbit (Cranston and Rosendorff, 1969), and cerebral cortex of anesthetized cats and dogs (Betz et al., 1966).

Sensitivity to Parameters

The temperature response resulting from dynamic temperature-forcing at a probe implanted in living brain tissue was described by a differential equation (equation 3), expressing heat transport in terms of heat conduction in tissue and heat convection due to blood flow. We feel that such a mathematical formulation has, primarily, two physiological applications: (*a*) the prediction of thermal gradients surrounding heated or cooled probes, and (*b*) the measurement of local tissue perfusion. In either case, the sensitivity of the solution of equation 3 to the parameters (k and ϕ') and the boundary conditions must be investigated. The effect of changes in k and ϕ' on the numerical solution of equation 3 is shown in Fig. 4. An increase in k (at constant ϕ') has the effect of increasing the initial slope and the steady-state value of the step response (Fig. 4 A). In the frequency domain (Fig. 4 B) an increase in k results in an increase in gain at all frequencies; the effect, however, is more pronounced at the higher frequencies. A decrease in k has the inverse effect.

Although k affects both the high and low frequency gain, changes in ϕ' are ap-

FIGURE 4 Effect of changes in k and ϕ' on the numerical solution of equation 3. Step responses for different values of k (ϕ' constant) are shown in A and for different values of ϕ' (k constant) in C. Experimental response is shown as a solid line. Sinusoidal responses for different values of k are shown in B and for different values of ϕ' in D. Experimental response is shown as hexagons. The coordinates of the tissue thermocouple were $r = 2.59$ mm and $z = 1.90$ mm.

parent only at the low frequencies. Thus an increase in ϕ' (at constant k) has little effect on the initial slope of the step response but causes a decrease in the steady-state values (Fig. 4 C). This can be seen in the frequency domain (Fig. 4 D) where an increase in ϕ' results in a decrease in the low frequency gain but no change at the higher frequencies. A decrease in ϕ' has the inverse effect.

These results indicate that for a given time-varying experimental response, independent values for k and ϕ' can be determined. It is also evident that relatively large changes in k and ϕ' have little effect on the temperature response, suggesting that equation 3 could be useful for determining temperature responses even when those parameters are not exactly known. However, the relative insensitivity of the solution to k, and especially ϕ', suggest that the utility of using equation 3 for the determination of local blood flow is limited.

Role of Capillary Convection

As noted earlier, convective heat transport can be considered as the result of two additive effects: capillary heat convection and forced convection (see equation 2). In the preceding discussion, the effect of capillary heat convection was assumed to be negligible. Since capillary heat convection is dependent on vessel orientation as well as blood flow, an accurate determination of the magnitude of the effect is difficult. However, the maximum contribution to heat transport from this source can be evaluated, assuming all capillaries are radially oriented with respect to the thermode. This situation is treated in Appendix I. A knowledge of average capillary length $\bar{l}_c$, in addition to ϕ' and k, is required for solution of the resulting equation,

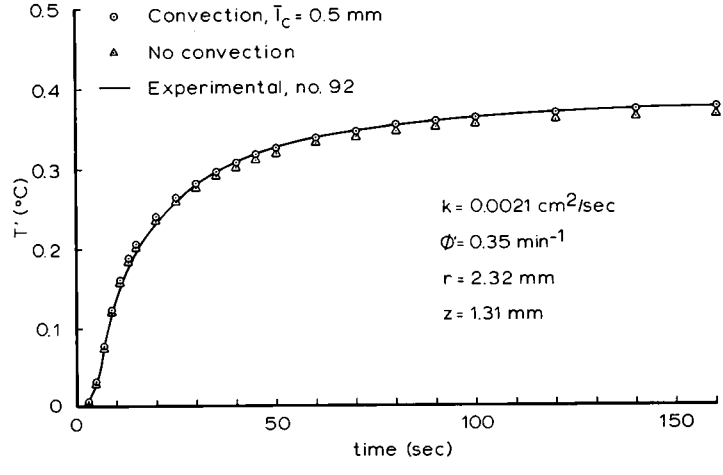

FIGURE 5 A comparison between the numerical solution of equation 3, assuming no capillary heat convection (triangles) and equation A 3, assuming convection for radially oriented capillaries (circles). Values of k and ϕ' shown were the same for both solutions. Coordinates of the tissue thermocouple are shown on the figure.

equation A 3. A comparison between the numerical solution of equation 3 and equation A 3 is shown in Fig. 5. A value of 0.5 mm was used for $\bar{l}_c$ (Reneau et al., 1967; Wiedeman, 1963; Smaje et al., 1970; Davis and Lawler, 1958), and the choice of k (0.0021 cm^2/sec) and ϕ' (0.35 min^{-1}) provided a visual best fit between the experimental data and the numerical solution for equation A 3. Although not illustrated, the solution of equation 3 (with no capillary convection term) will also fit the experimental data using the same value of k but with $\phi' = 0.28$ min^{-1}. Since these solutions represent extreme cases, the calculated value of ϕ' will fall somewhere between 0.28 and 0.35 min^{-1} if the capillary convection is included, but cannot be determined uniquely without additional information about capillary orientation and blood flow. Although the addition of the capillary heat convection term has a significant effect on the value of ϕ' required to fit the experimental data, Fig. 5 shows that addition of this term results in a relatively small change in the temperature response.

Evaluation of Tissue Damage

In previous sections both blood flow and thermal properties were assumed to be the same throughout the tissue. However, as illustrated in Fig. 3, it is evident that introduction of the thermode needles into the brain results in considerable tissue damage. The region occupied by scar tissue approximates an annulus surrounding the needles varying in thickness from almost zero to greater than 1 mm. Since this scar tissue consists primarily of glial cells and contains few fibrous components, its thermal diffusivity (k), density (ρ), and specific heat (c) were assumed equal to that

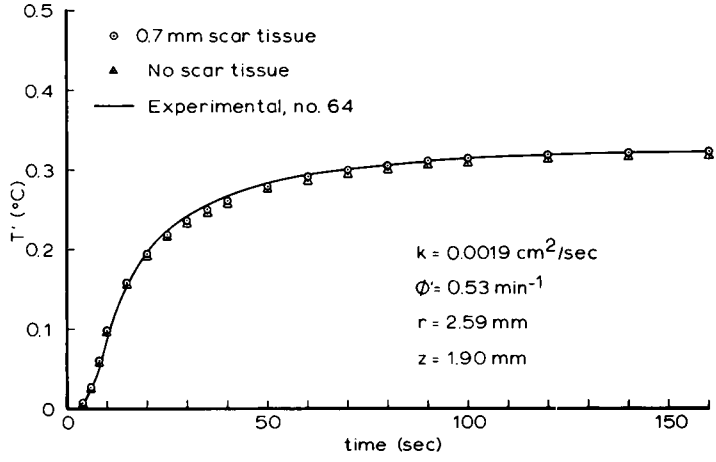

FIGURE 6 A comparison between the numerical solution of equation 3 assuming 0.7 mm of avascular scar tissue surrounds the thermode needle (circles), and assuming no scar tissue (triangles). The experimental response is shown as a solid line. Values of k and ϕ' were the same for both solutions.

of normal brain tissue. It has been reported, however, that vascularity of scar tissue surrounding old brain lacerations is greatly reduced (Alexander and Putnam, 1937). Thus, an attempt was made to investigate the effect of scar tissue on the numerical solution of equation 3 using the following assumptions: (*a*) The scar tissue occupies a 0.7 mm annulus surrounding the thermode needles. (*b*) Thermal properties (k, ρ, c) are the same for both normal and scar tissue. (*c*) Blood flow in the scar tissue is zero (representing the extreme case). A comparison between the numerical solution of equation 3 with and without scar tissue is shown in Fig. 6. Values of k and ϕ' were chosen to provide a visual best fit between experimental and theoretical data assuming the presence of avascular scar tissue. As previously shown in Fig. 4, the solution of equation 3 (assuming no scar tissue) will also fit this experimental data using the same value of k but with $\phi' = 0.48$ min^{-1}. Although the difference in ϕ' is relatively small, these results indicate that no unique value can be determined without more information about the vascularity of scar tissue.

In addition to scar tissue, nonuniformities in blood flow distribution occur due to differences in vascularity of gray and white matter (James et al., 1969; Craigie, 1920). Since little quantitative information about blood flow distribution in the hypothalamus is available, and since the geometry is difficult to handle mathematically, no attempt was made to evaluate the effect due to regional blood flow differences.

Sensitivity to Boundary Conditions

It was noted earlier that solution of a differential equation, such as equations 3 or A 3, requires knowledge of certain boundary conditions. When these equations are expressed in cylindrical coordinates, the temperature for all time at specific radial and axial coordinates must be defined. For the equations under study, no choice is available for the inner radial (thermode) boundary condition (equation A 5 *a*). However, the choice of the outer radial boundary and both axial boundaries (equations A 5 *b*, *d*, and *e*) is determined by the geometry of the brain surface. It was found, though, that these boundaries could be much closer to the thermode than the brain surface without significantly affecting the solution in the vicinity of the thermode tip; the outer boundaries were chosen accordingly (Appendix II). Thus the complex geometry of the surface of the brain appears to have little effect near the thermode because of the steepness of the temperature gradients in this region.

Predicted Temperature Distribution

The previous results indicate that good agreement between computed and experimental results was obtained in both the time and frequency domain, and these results were not greatly affected by variations in the parameters and outer boundary conditions. Although temperature was not measured simultaneously at different tissue locations, the data from the three animals represent measurements at three

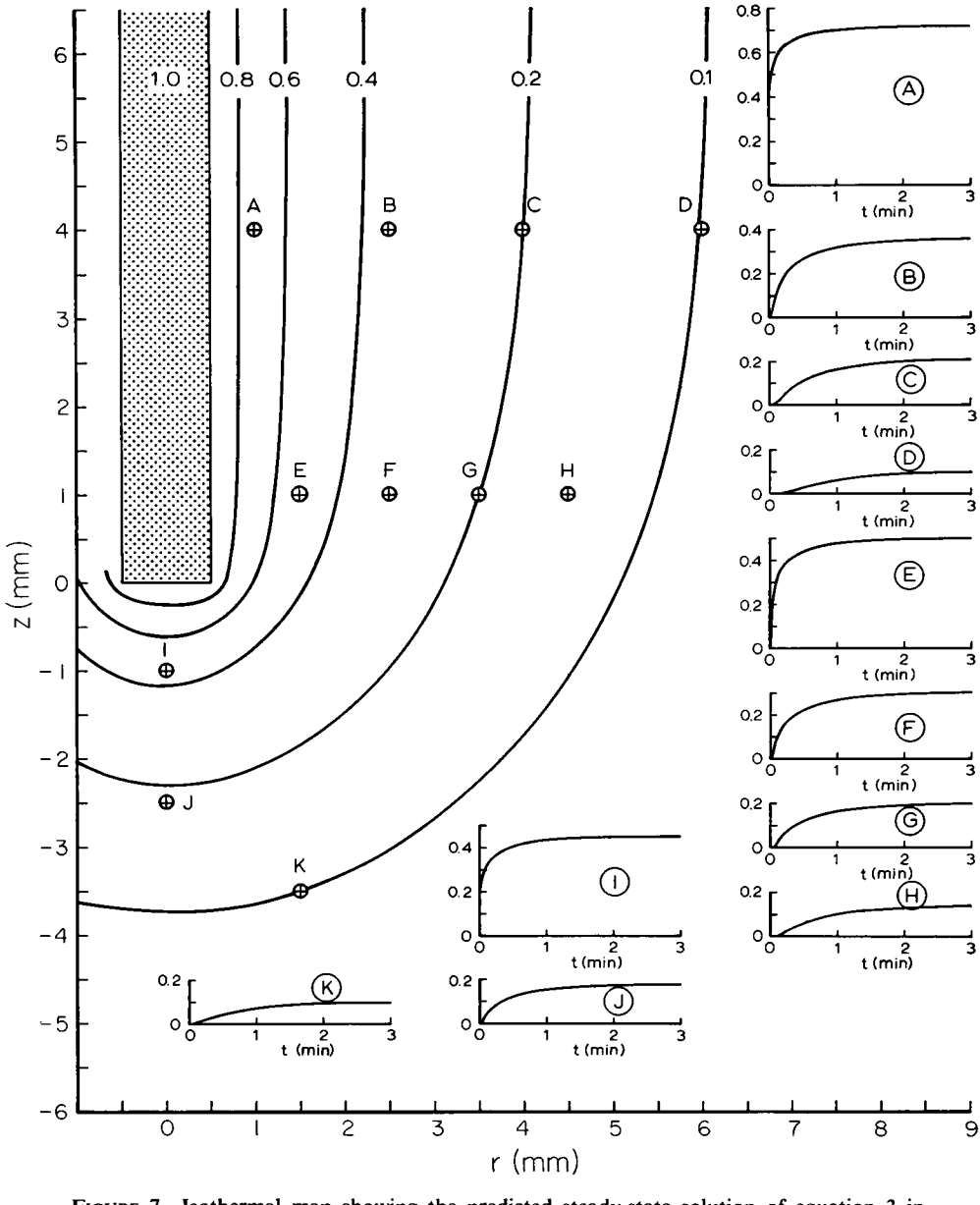

FIGURE 7 Isothermal map showing the predicted steady-state solution of equation 3 in response to a 1°C step increase in temperature of a 1 mm O.D. thermode. The inserts (letters A–K) illustrate the predicted temperature changes as a function of time for various tissue locations. Values of k and ϕ' were 0.0019 and 0.48 min^{-1} respectively.

different tissue coordinates. Thus, it seemed reasonable to use the numerical solution of equation 3 to predict the thermal response at other tissue locations. A solution was computed for a 1°C step increase in temperature at a 1 mm O.D. thermode assuming $k = 0.0019$ cm^2/sec and $\phi' = 0.48$ min^{-1}. Fig. 7 illustrates both the steady-state values (in the form of an isothermal map) and the time responses at several points in the tissue. This figure emphasizes the steep thermal gradients resulting from localized heating and shows the slow time course of the temperature response.

CONCLUSIONS

A partial differential equation describing heat transport in terms of heat conduction in a homogeneous medium, and convection due to blood flow, has been used to describe dynamic temperature responses around cylindrical thermodes chronically implanted in brain tissue. Proper selection of the parameters k (thermal diffusivity) and ϕ' (adjusted blood flow) resulted in good agreement between theoretical and experimental data in either the time or frequency domain. However, no unique set of parameters describes the experimental data since simply adjusting the value of ϕ' allows a fit between experimental and theoretical results when the assumption of avascular scar tissue or the assumption of capillary heat convection was included in the equation.

The effect of including scar tissue or capillary heat convection on the temperature response was relatively small, despite the fact that extreme cases were assumed. Fortunately, for a particular formulation, moderate changes in k and ϕ' over the physiological range also had little effect on the predicted temperature response. Thus, it can be concluded that any of these formulations are adequate to predict time-varying, as well as steady-state, temperature fields in living brain tissue surrounding cylindrical thermodes.

We may conclude the following regarding the potential utility of thermal measurements in evaluating regional brain blood flow. First, the calculated value of ϕ' required to fit the experimental data is sensitive to assumptions regarding capillary heat convection and conduction through scar tissue. Thus, the contribution of capillary convection and scar tissue conduction must be measured experimentally before the calculated value of ϕ' can be associated with actual blood flow. Second, the actual temperature pattern is relatively insensitive to changes in ϕ'. Therefore, tissue temperature must be precisely measured in order to accurately estimate tissue perfusion. Furthermore, ϕ' affects primarily the steady-state temperature response, which requires that the blood flow remain constant for a period of at least 2–3 min for a determination of tissue perfusion. Thus, the utility of this method is probably limited to qualitative measurements of steady-state blood flow and cannot be used for quantitative or instantaneous determination of tissue perfusion.

This study was supported in part by National Institutes of Health grants GM 00739-13, FR 00166 5-F01-GM-30, 983, and by United States Air Force contract F 33615696-1306.

Received for publication 13 October 1970 and in revised form 21 January 1971.

REFERENCES

ALEXANDER, L., and T. J. PUTNAM. 1937. *In* The Circulation of the Brain and Spinal Cord. S. Cobb, A. M. Frantz, W. Penfield, and H. A. Riley, editors. Hafner Publishing Co., Inc., New York.

BETZ, E. 1965. *Acta Neurol. Scand. Suppl.* **14**:29.

BETZ, E., D. H. INGVAR, N. A. LASSEN, and F. W. SCHMAHL. 1966. *Acta Physiol. Scand.* **67**:1.

BROWN, A. C. 1965. *Bull. Math. Biophys.* **27**:67.

CARLSLAW, H. S., and J. C. JAEGER. 1959. *In* Conduction of Heat in Solids. Clarendon Press, Oxford, England.

CHATO, J. C., and SHITZER. 1970. Proceedings of Conference on Engineering in Medicine and Biology, Washington, D.C.

COOPER, T. E., and G. J. TREZEK. 1970. Proceedings of Conference on Engineering in Medicine and Biology, Washington, D.C.

CRAIGIE, E. H. 1920. *J. Comp. Neurol.* **31**:429.

CRANSTON, W. I., and ROSENDORFF. 1969. *J. Physiol. (London).* **204**:25P.

DAVIS, M. J., and J. C. LAWLER. 1958. *A.M.A. Arch. Dermatol.* **77**:690.

GIBBS, F. A. 1933. *Proc. Soc. Exp. Biol. Med.* **31**:141.

GRAYSON, J. 1952. *J. Physiol. (London).* **118**:54.

HAMMING, R. W. 1962. Numerical Methods for Scientists and Engineers. McGraw-Hill Book Company, New York.

JAMES, I. M., R. A. MILLAR, and M. J. PURVES. 1969. *Circ. Res.* **25**:77.

JEWETT, D. L., and G. J. TREZEK. 1967. Proceedings of 20th Conference on Engineering in Medicine and Biology.

KASTELLA, K. G. 1970. *J. Appl. Physiol.* **29**:508.

KUNZ, K. S. 1957. Numerical Analysis. McGraw-Hill Book Company, New York.

MENDLOWITZ, M. 1948. *Science (Washington).* **107**:97.

PERL, W. 1962. *J. Theor. Biol.* **2**:201.

PONDER, E. 1962. *J. Gen. Physiol.* **45**:545.

RENEAU, D. D., D. F. BRULEY, and M. H. KNISELEY. 1967. Chemical Engineering in Medicine and Biology. D. Hershey, editor. Plenum Publishing Corporation, New York.

RUTKIN, B. B., and E. Z. BARISH. 1964. Proceedings of 17th Conference on Engineering in Medicine and Biology.

SMAJE, L., B. W. ZWEIFACH, and M. INTAGLIETTA. 1970. *Microvasc. Res.* **2**:96.

TREZEK, G. J., D. L. JEWETT, and T. E. COOPER. 1968. Proceedings of 1968 Thermal Conductivity Conference. D. R. Flynn and B. A. Peary, editors. *Nat. Bur. Stand. (U.S.) Spec. Publ.* 302.

WIEDEMAN, M. P. 1963. *Circ. Res.* **12**:375.

APPENDIX I

Heat Transport Due to Conduction

The accumulation of heat per unit volume of tissue due to conduction can be expressed as (Carlslaw and Jaeger, 1959):

$$\frac{\partial}{\partial t}\rho cT = \text{div } K \text{ grad } T \text{ (cal/cm}^3\text{-sec)}.$$

If ρ and c are assumed to be time-invariant and K is assumed to be space-invariant, this expression becomes

$$\frac{\partial T}{\partial t} = k \text{ div grad } T \text{ (°C/sec)},$$

where $k = K/\rho c$.

Heat Transport Due to Convection

Heat convection due to capillary blood flow depends on the geometry of the capillary bed. on blood flow in each capillary, and on the density and specific heat of the blood in each capillary. A quantitative description of these factors is nearly impossible. However, the heat convection for the case where all capillaries are parallel and with blood flow in the same direction can be computed to give an estimate of the maximum effect on heat transport (Perl, 1962). If a small cubic volume of tissue containing parallel but randomly located capillaries is considered, where

l = length of a side of the volume element (cm),
n = total number of capillaries in the volume,
n_p = average number of capillaries crossing a plane (area l^2) placed perpendicular to the axis of the capillaries,
F_i = flow in the ith capillary, $1 \leq i \leq n$ (cm³/sec),
F = total arterial-to-capillary blood flow in the volume element (cm³/sec),
l_{c_i} = length of the ith capillary (cm),
$\bar{l}_c$ = average capillary length (cm);

thus, the total capillary blood flow within the element is assumed to be:

$$\sum_{i=1}^{n} F_i = F = \phi l^3 \text{ (cm}^3\text{/sec)},$$

and the total blood flow through a plane perpendicular to the axis of the capillaries will be:

$$\sum_{j=1}^{n} F_j \text{ (cm}^3\text{/sec)},$$

where the subscript j refers to only those capillaries that cross the plane. If it is assumed that the average flow for all capillaries in the volume is equal to the average flow in capillaries crossing the plane, i.e.:

$$\frac{1}{n}\sum_{i=1}^{n} F_i = \frac{1}{n_p}\sum_{j=1}^{n_p} F_j \text{ (cm}^3\text{/sec)},$$

then the total blood flow through the plane is:

$$\sum_{j=1}^{n_p} F_j = \frac{n_p}{n}\sum_{i=1}^{n} F_i = \frac{n_p}{n} F \text{ (cm}^3\text{/sec)},$$

and flow per unit area across the plane is:

$$\frac{n_p}{n}\frac{F}{l^2} \text{ (cm}^3\text{/cm}^2\text{-sec)}.$$

If it is also assumed that the probability of the ith capillary crossing the plane is l_{c_i}/l, then the average number of capillaries crossing the plane will be:

$$n_p = \sum_{i=1}^{n} \frac{l_{c_i}}{l} = \frac{n}{l}\frac{1}{n}\sum_{i=1}^{n} l_{c_i} = \frac{n}{l}\bar{l}_c.$$

If T_b is the temperature of the capillary blood as it crosses the plane, the heat flux across the plane due to convection will be:

$$\rho_b c_b T_b \frac{n_p}{n} \frac{F}{l^2} = \rho_b c_b T_b \bar{l}_c \text{ (cal/cm}^2\text{-sec)}.$$

Assuming that ρ_b, c_b, and $\bar{l}_c$ are spatially invariant, that the capillary blood is the same temperature as the surrounding tissue, and that div $\phi = 0$, the accumulation of heat per unit volume of tissue due to convection will be:

$$\rho c \frac{\partial T}{\partial t} = - \text{ div } \rho_b c_b \bar{l}_c \phi T = - \rho_b c_b \bar{l}_c \phi \text{ grad } T \text{ (cal/cm}^3\text{-sec)}.$$

The accumulation of heat per unit volume of tissue due to equilibration of arterial blood (entering the tissue element at temperature T_a) with the tissue (temperature T) can be expressed as:

$$\rho c \frac{\partial T}{\partial t} = \rho_b c_b \phi (T_a - T) \text{ (cal/cm}^3\text{-sec)}.$$

Arterial blood density and specific heat are assumed to be the same as for capillary blood.

The Combined Equation

Combining the effects of conduction, convection and metabolism yields the equation:

$$\frac{\partial T}{\partial t} = k \text{ div grad } T - \phi' \bar{l}_c \text{ grad } T + \phi' (T_a - T) + \frac{h_m}{\rho c}. \qquad \text{(A 1)}$$

An initial unforced temperature distribution $\left(\frac{\partial T_0}{\partial t} = 0\right)$, T_0, can be defined such that:

$$0 = k \text{ div grad } T_0 - \phi' \bar{l}_c \text{ grad } T_0 + \phi' (T_a - T) + \frac{h_m}{\rho c}. \qquad \text{(A 2)}$$

If metabolism h_m and blood flow ϕ are assumed constant in time, and if the substitution $T' = T - T_0$ is made in equation A 1, the resulting equation can be subtracted from equation A 2, yielding:

$$\frac{\partial T'}{\partial t} = k \text{ div grad } T' - \bar{l}_c \phi' \text{ grad } T' - \phi' T', \qquad \text{(A 3)}$$

where T' represents the change in temperature at any point in the tissue.

Equation A 3 can be expressed in cylindrical coordinates; assuming radial symmetry, the response to thermode heating becomes:

$$\frac{\partial T'}{\partial t} = k \frac{\partial^2 T'}{\partial r^2} + \frac{k}{r} \frac{\partial T'}{\partial r} - \bar{l}_c \phi' \frac{\partial T'}{\partial r} - \phi' T' + k \frac{\partial^2 T'}{\partial z^2}. \qquad \text{(A 4)}$$

The boundary conditions for a cylindrical thermode with axis at $r = 0$ and tip located at $z = 0$ are:

$$T'(r_1, z, t) = f(t),\ t \geq 0,\ z \geq 0, \tag{A 5 a}$$

$$T'(r_2, z, t) = 0, \tag{A 5 b}$$

$$\frac{\partial T'}{\partial r} = 0,\ r = 0,\ z < 0, \tag{A 5 c}$$

$$T'(r, z_1, t) = 0, \tag{A 5 d}$$

$$T'(r, z_2, t) = 0, \tag{A 5 e}$$

and the initial condition is:

$$T'(r, z, 0) = 0, \tag{A 5 f}$$

where

r_1 = thermode radius,
r_2 = outer radial boundary coordinate,
z_1 = lower axial boundary coordinate,
z_2 = upper axial boundary coordinate, and
$f(t)$ = temperature at thermode surface.

APPENDIX II

The finite difference equation used to approximate equation A 4 was:

$$\begin{aligned}\frac{T'_{i,j,m+1} - T'_{i,j,m}}{h} = {} & \frac{k}{p^2}\left(T'_{i+1,j,m} - 2T'_{i,j,m} + T'_{i-1,j,m}\right) \\ & + \frac{k}{2pr_i}\left(T'_{i+1,j,m} - T'_{i-1,j,m}\right) \\ & - \frac{\bar{l}_c\phi'}{2p}\left(T'_{i+1,j,m} - T'_{i-1,j,m}\right) \\ & - \phi' T'_{i,j,m} + \frac{k}{b^2}\left(T'_{i,j+1,m} - 2T'_{i,j,m} + T'_{i,j-1,m}\right),\end{aligned} \tag{A 6}$$

where $T'_{i,j,m} = T'(r_i, z_i, t_m)$,

$r_i = r_1 + ip,\ 0 \leq i \leq 30;$

$z_j = jb,\ -22 \leq j \leq 30;$

$t_m = mh,\ 0 \leq m \leq 1000;$

and i, j, m are integers. Spacing in the time direction (h) was 0.25 sec. Spacing in the r- and

z-directions (p and b) was chosen so that a value of r_i and z_i would coincide with the coordinates of the remote thermocouple. Values for p and b were always between 0.04 and 0.06 cm. The unequal grid spacing between $r = 0$ and $r = r_1$ was accounted for by using a quadratic interpolation formula. The difference equation used for solution of equation 3 was identical to A 6 but with $l_c = 0$.

The boundary conditions (equations A 5 *a–f*) expressed as difference equations were:

$$T'(r_1, z_j, t_m) = f(t_k),\ j \geq 0; \qquad T'(r_i, z_{30}, t_m) = 0,$$

$$\left.\frac{\partial T'}{\partial t}\right|_{0,j,m} = 0,\ j < 0; \qquad T'(r_i, z_{-22}, t_m) = 0,$$

$$T'(r_i, z_j, 0) = 0.$$

$$T'(r_{30}, z_j, t_m) = 0,$$

The difference equation, equation A 6, was solved for $T'_{i,j,m+1}$ and used to compute successive values of $T'_{i,j,m+1}$ from values of $T'_{i,j,m}$, $T'_{i+1,j,m}$, $T'_{i-1,j,m}$, $T'_{i,j+1,m}$, and $T'_{i,j-1,m}$. This "marching" technique (Kunz, 1957) computes new points in time from previous points and from boundary conditions. Values of T' were computed for 30 points in the radial direction, 53 points in the axial direction, and 1000 points (250 sec) in the time direction. Values for p, b, and h were sufficient to assure stability of the solution (Kunz, 1957).